
Early Treatment Response Assessment Using ^{18}F -FET PET Compared with Contrast-Enhanced MRI in Glioma Patients After Adjuvant Temozolomide Chemotherapy

Garry Ceccon¹, Philipp Lohmann², Jan-Michael Werner¹, Caroline Tscherpel^{1,2}, Veronika Dunkl¹, Gabriele Stoffels², Jurij Rosen¹, Marion Rapp³, Michael Sabel³, Ulrich Herrlinger^{4,5}, Niklas Schäfer^{4,5}, Nadim J. Shah^{2,6}, Gereon R. Fink^{1,2}, Karl-Josef Langen^{2,5,7}, Norbert Galldiks^{1,2,5}

¹Department of Neurology, Faculty of Medicine and University Hospital Cologne, University of Cologne, Germany; ²Institute of Neuroscience and Medicine (INM-3, -4), Research Center Juelich, Juelich, Germany; ³Department of Neurosurgery, University Hospital Duesseldorf, Duesseldorf, Germany; ⁴Division of Clinical Neurooncology, Department of Neurology, University Hospital Bonn, Bonn, Germany; ⁵Center of Integrated Oncology (CIO), Universities of Aachen, Bonn, Cologne, and Duesseldorf, Aachen and Cologne, Germany; ⁶Department of Neurology, University Hospital Aachen, Aachen, Germany; and ⁷Department of Nuclear Medicine, University Hospital Aachen, Aachen, Germany

Background: The goal of this study was to compare the value of contrast-enhanced MRI and O-(2-[^{18}F]fluoroethyl)-L-tyrosine (^{18}F -FET) PET for response assessment in glioma patients after adjuvant temozolomide chemotherapy (TMZ). **Methods:** After biopsy or resection and completion of radiotherapy with concomitant TMZ, 41 newly diagnosed and histomolecularly characterized glioma patients (glioblastoma, 90%; age range, 20–79 y) were subsequently treated with adjuvant TMZ. MR and ^{18}F -FET PET imaging were performed at baseline and after the second cycle of adjuvant TMZ. We obtained ^{18}F -FET metabolic tumor volumes (MTVs) as well as mean and maximum tumor-to-brain ratios (TBR_{mean} and TBR_{max}, respectively). Threshold values of ^{18}F -FET PET parameters to predict outcome were established by receiver-operating-characteristic analyses using a median progression-free survival (PFS) of ≥ 9 mo and overall survival (OS) of ≥ 15 mo as reference. MRI response assessment was based on the Response Assessment in Neuro-Oncology (RANO) working group criteria. The predictive value of changes of ^{18}F -FET PET and MRI parameters on survival was evaluated subsequently using univariate and multivariate survival estimates. **Results:** After 2 cycles of adjuvant TMZ chemotherapy, a treatment-induced reduction of MTV and TBR_{max} predicted a significantly longer PFS and OS (both $P \leq 0.03$; univariate survival analyses) whereas RANO criteria were not significant ($P > 0.05$). Multivariate survival analysis revealed that TBR_{max} changes predicted a prolonged PFS ($P = 0.012$) and changes of MTV a prolonged OS ($P = 0.005$) independent of O⁶-methylguanine-DNA-methyltransferase promoter methylation and other strong prognostic factors. **Conclusion:** Changes of ^{18}F -FET PET parameters appear to be helpful for identifying responders to adjuvant TMZ early after treatment initiation.

Key Words: amino acid PET; treatment monitoring; treatment-related changes; pseudoprogression; metabolic tumor volume;

J Nucl Med 2021; 62:918–925

DOI: 10.2967/jnumed.120.254243

The prognosis of patients with glioblastoma is still relatively poor, with median overall survival (OS) rates ranging between 15 and 20 mo (1–3). Since 2005, first-line treatment has consisted of cytoreductive surgery, followed by radiotherapy with concomitant and adjuvant temozolomide (TMZ) chemotherapy, according to the EORTC-NCIC 22981/26981 protocol (1). More recently, in glioblastoma patients, further survival benefit has been achieved by adding tumor-treating fields concurrent to adjuvant TMZ chemotherapy (4,5), or by lomustine/TMZ combination chemotherapy in glioblastoma patients with O⁶-methylguanine-DNA-methyltransferase (MGMT) promoter methylation (6). Nevertheless, in many centers, radiotherapy with concomitant and adjuvant TMZ is still the standard of care.

For decades, the method of choice for treatment response assessment in brain tumor patients was contrast-enhanced anatomic MRI. Predominantly, changes of contrast enhancement are used as a surrogate of treatment response or tumor progression (7,8). However, contrast enhancement resulting from increased blood–brain barrier permeability is nonspecific and may not always be an accurate indicator of neoplastic tissue, tumor extent, or treatment effect (9–11). Importantly, since the introduction of chemoradiation with TMZ, there has been an increasing awareness of progressive enhancing lesions on MRI, which are related to the treatment. These findings eventually either remain stable or may ultimately even regress, as observed during follow-up MRI without any change of treatment. Accordingly, this phenomenon was termed pseudoprogression (12–14). Typically, this phenomenon occurs within the first 12 wk after chemoradiation completion (7) and may also occur beyond the 12-wk time window (15,16). Similarly, radiation necrosis, which usually manifests several months later than pseudoprogression, may also lead to contrast enhancement on MRI (17). Additionally, nonspecific contrast enhancement may result from postoperative inflammation, ischemia, and seizures (18,19). Consequently, alternative diagnostic methods are needed to improve the evaluation of treatment response.

In the recent past, numerous studies have shown that PET using the radiolabeled amino acid O-(2-[^{18}F]fluoroethyl)-L-tyrosine (^{18}F -FET) provides valuable additional diagnostic information for various indications in neurooncology, including the assessment of

Received Jul. 28, 2020; revision accepted Oct. 8, 2020.

For correspondence or reprints, contact Norbert Galldiks (n.galldiks@fz-juelich.de).

Published online Nov. 6, 2020.

COPYRIGHT © 2021 by the Society of Nuclear Medicine and Molecular Imaging.

treatment response (20,21). Moreover, the Response Assessment in Neuro-Oncology (RANO) working group has emphasized that for gliomas and brain metastases, the additional clinical value of amino acid PET compared with standard MRI is excellent as it provides valuable diagnostic information for treatment response assessment (22,23).

However, studies evaluating the value of ^{18}F -FET PET for treatment response assessment in glioma patients (24–27) are predominantly based on mostly heterogeneous patient groups (i.e., usually heavily pretreated glioma patients with different histomolecular diagnoses or inconsistent imaging time points). Additionally, very few studies have addressed the value of ^{18}F -FET PET only for the assessment of response to chemoradiation with concurrent TMZ in newly diagnosed glioblastoma patients treated according to the EORTC/NCIC 22981/26981 trial (28–30).

To evaluate the response to adjuvant TMZ chemotherapy using ^{18}F -FET PET and contrast-enhanced MRI, we performed a study in newly diagnosed glioma patients. We aimed to identify which ^{18}F -FET PET parameter in comparison to MRI is best suited for predicting a significantly longer survival early after adjuvant TMZ treatment initiation.

MATERIALS AND METHODS

Patients

From 2015 to 2019, we examined 41 consecutive adult patients (mean age, 52 ± 13 y; age range, 20–79 y; 19 women) with a Karnofsky performance status $\geq 70\%$ and newly diagnosed glioma (predominantly glioblastoma, 90%) using MR and ^{18}F -FET PET imaging. All patients underwent resection or stereotactic biopsy and had histomolecularly confirmed gliomas and completed radiotherapy with concomitant TMZ chemotherapy according to the EORTC/NCIC 22981/26981 trial (1). Neuroimaging was performed at baseline (within 7 d before adjuvant TMZ initiation) and after the second cycle of adjuvant TMZ. Further details on the patients' characteristics are listed in Table 1.

Treatment and Follow-up

After resection or biopsy, all patients were treated with radiotherapy (60 Gy) and concomitant and adjuvant TMZ chemotherapy over 6 cycles according to the EORTC/NCIC 22981/26981 trial (1). Contrast-enhanced conventional MRI was performed within the first 48 h after resection and every 8–12 wk. Patients were assessed by neurologic examination and the Karnofsky performance score at baseline and every 8–12 wk during the treatment and after treatment completion. The patients' outcome was prospectively followed. The progression-free survival (PFS) was defined as the time interval between histomolecularly confirmed glioma diagnosis and tumor progression according to RANO criteria (7). The OS was defined as the time interval between histomolecularly confirmed glioma diagnosis and death.

Conventional MR Imaging

In accordance with the International Standardized Brain Tumor Imaging Protocol (31), MRI was performed using a 1.5-T or 3.0-T MRI scanner with a standard head coil before and after administration of a gadolinium-based contrast agent (0.1 mmol/kg body weight). The sequence protocol comprised 3-dimensional (3D) isovoxel T1-weighted, 2-dimensional (2D) T2-weighted, and 2D fluid-attenuated inversion recovery-weighted sequences. MRI changes at first follow-up compared with the baseline scan were assigned according to the RANO criteria (7). The criteria for stable disease, partial response, and complete response were considered for assessing the response to treatment.

^{18}F -FET PET Imaging

As described previously, the amino acid ^{18}F -FET was produced via nucleophilic ^{18}F -fluorination with a radiochemical purity of greater than 98%, molar radioactivity greater than 200 GBq/ μmol , and a radiochemical yield of about 60% (32). According to international guidelines for brain tumor imaging using labeled amino acid analogs (33), patients fasted for at least 4 h before the PET measurements. All patients underwent a dynamic PET scan from 0 to 50 min after injection of 3 MBq of ^{18}F -FET per kg of body weight at baseline (within 7 d before starting of adjuvant TMZ) and after the second cycle of adjuvant TMZ. PET imaging was performed either on an ECAT Exact HR+ PET scanner in 3D mode ($n = 64$ scans; Siemens; axial field of view, 15.5 cm) or simultaneously with 3T MRI using a BrainPET insert ($n = 15$ scans; Siemens; axial field of view, 19.2 cm). The BrainPET is a compact cylinder that fits into the bore of the Magnetom Trio MR scanner (34).

Iterative reconstruction parameters were 16 subsets, 6 iterations using the ordered-subset expectation maximization (OSEM) algorithm for the ECAT HR+ PET scanner and 2 subsets, 32 iterations using the ordinary Poisson-OSEM algorithm for the BrainPET. Data were corrected for random and scattered coincidences, dead time, and motion for both systems. Attenuation correction for the ECAT HR+ PET scan was based on a transmission scan, and for the BrainPET scan on a template-based approach (34). The reconstructed dynamic datasets consisted of 16 time frames (5×1 min; 5×3 min; 6×5 min) for both scanners.

To optimize the comparability of the results related to the influence of the 2 different PET scanners, reconstruction parameters, and postprocessing steps, a 2.5-mm 3D gaussian filter was applied to the BrainPET data before further processing. In phantom experiments using spheres of different sizes to simulate lesions, this filter kernel demonstrated the best comparability between PET data obtained from the ECAT HR+ PET and the BrainPET scanner (35).

^{18}F -FET PET Data Analysis

For the evaluation of ^{18}F -FET data, summed PET images over 20–40 min after injection were used. Mean tumoral ^{18}F -FET uptake was determined by a 2D auto-contouring process using a tumor-to-brain ratio (TBR) of at least 1.6. This cutoff was based on a biopsy-controlled study in glioma patients and differentiated best between tumoral and peritumoral tissue (36). A circular region of interest (ROI) with a diameter of 1.6 cm was centered on the maximal tumor uptake for the evaluation of the maximal ^{18}F -FET uptake, as previously reported (37). Mean and maximum TBRs (TBR_{mean} and TBR_{max}, respectively) were calculated by dividing the mean and maximum SUV of the tumor ROI by the mean SUV of a larger ROI placed in the semioval center of the contralateral unaffected hemisphere including white and gray matter (33). The calculation of ^{18}F -FET metabolic tumor volumes (MTVs) was determined by a 3D auto-contouring process using a threshold of 1.6, using PMOD (version 3.505; PMOD Technologies Ltd.).

Neuropathologic Tumor Classification and Analysis of Molecular Markers

All tumors were histomolecularly classified according to the World Health Organization (WHO) Classification of Tumors of the Central Nervous System of 2016 (38). For molecular biomarker analysis, tumor DNA was extracted from formalin-fixed and paraffin-embedded tissue samples with a histologically estimated tumor cell content of 80% or more. For assessment of the isocitrate dehydrogenase (IDH) mutation status, the presence of an IDH1-R132H mutation was evaluated by immunohistochemistry using a mutation-specific antibody in a standard immunohistochemical staining procedure as reported (39,40). If immunostaining for IDH1-R132H remained negative, the mutational hot spots

TABLE 1
Patient Characteristics and Neuroimaging Findings

Patient	Sex	Age at Dx	MGMT promoter methylation	IDH mutation	Dx	EOR	MTV BL (mL)	MTV FU (mL)	TBR _{mean} BL	TBR _{mean} FU	TBR _{max} BL	TBR _{max} FU	MRI res	PFS (mo)	OS (mo)
1	M	66	meth	wt	GBM	B	42.8	20.8	2.3	2.2	3.1	2,5	PD	16	29
2	M	47	meth	wt	GBM	B	10.7	20.2	2.0	2.2	2.0	2.6	SD	16	21
3	M	62	meth	wt	GBM	CR	5.2	4.3	1.9	1.9	1.9	1.9	SD	11	31
4	M	76	meth	wt	GBM	B	95.5	n.a.	2.1	n.a.	2.8	n.a.	PD	3	5
5	M	69	not meth	wt	GBM	CR	3.4	4.1	1.8	1.8	1.8	1.8	SD	9	34
6	M	69	meth	wt	GBM	B	37.8	n.a.	1.9	n.a.	2.3	n.a.	SD	4	5
7	M	44	not meth	wt	GBM	PR	18.4	14.2	1.9	1.8	1.9	1.8	PD	11	17
8	F	50	meth	wt	GBM	B	8.4	15.8	1.9	1.9	2.4	2.6	SD	5	12
9	F	49	not meth	wt	GBM	PR	26.8	53.7	1.9	1.9	2.0	2.1	PD	11	12
10	F	58	meth	wt	GBM	B	4.3	4.3	2.0	1.9	2.0	1.9	SD	54*	54*
11	M	30	not meth	wt	GBM	PR	17.8	18.9	2.1	2.2	2.8	3.1	SD	8	14
12	M	54	not meth	wt	GBM	PR	60.7	101.0	1.8	2.1	2.0	2.3	PD	8	10
13	F	66	not meth	wt	GBM	B	103.2	137.1	2.6	2.2	4.4	3.2	PD	10	11
14	M	44	meth	mut	GBM	B	13.8	8.4	1.8	1.9	2.0	2.1	PD	15	54*
15	M	58	meth	wt	GBM	CR	43.6	82.1	1.9	2.0	2.1	2.3	SD	5	11
16	F	61	not meth	NOS	GBM	CR	44.1	44.5	2.3	2.4	2.8	3.2	PD	8	50
17	M	61	not meth	wt	GBM	B	29.7	38.3	2.2	2.2	2.5	3.1	PD	4	5
18	F	26	meth	wt	GBM	CR	2.4	0.7	1.9	1.8	1.9	1.8	SD	37	47*
19	F	51	not meth	wt	GBM	CR	1.8	4.5	1.8	1.8	1.8	1.8	PD	12	22
20	F	50	not meth	wt	GBM	CR	14.2	10.7	1.8	1.8	1.8	1.8	n.a.	10	10
21	M	59	not meth	NOS	GBM	PR	10.8	24.9	2.0	1.9	2.1	2.3	SD	7	10
22	M	39	not meth	wt	GBM	B	3.2	11.5	2.0	2.2	2.0	2.8	PD	5	10
23	F	54	meth	wt	AA	B	0.0	0.0	1.7	1.3	1.7	1.3	SD	30	31*
24	F	32	meth	mut	GBM	PR	3.6	14.9	2.2	1.8	2.2	1.8	PD	12	24
25	F	20	not meth	wt	H3K27 MPR		1.4	0.6	1.8	1.7	1.8	1.7	PD	18	31
26	M	66	meth	wt	AA	B	0.6	3.2	1.7	1.8	1.7	1.8	SD	11	16
27	M	46	not meth	wt	GBM	CR	12.7	14.7	1.9	2.0	1.9	2.1	SD	9	16
28	F	66	meth	wt	GBM	CR	13.5	9.3	1.8	1.8	1.9	1.9	PD	8	17
29	M	48	meth	mut	GBM	CR	14.6	5.6	1.9	1.8	2.1	1.8	PD	24*	24*
30	F	49	not meth	wt	GBM	CR	7.2	14.9	1.8	2.0	1.8	2.3	PD	11	22
31	M	38	not meth	wt	GBM	PR	75.5	40.2	1.8	1.9	2.3	2.5	SD	6	12
32	F	52	not meth	wt	GBM	PR	48.9	48.5	2.5	2.3	3.5	3.0	PD	4	13
33	M	46	meth	wt	GBM	B	2.6	n.a.	1.8	n.a.	1.8	n.a.	SD	4*	8
34	F	68	not meth	wt	GBM	PR	41.6	26.3	2.0	1.8	2.0	1.8	PD	7	15
35	M	79	not meth	wt	GBM	B	58.0	59.0	2.3	2.1	3.2	2.4	PD	6	6
36	F	43	not meth	wt	GBM	B	67.0	54.0	2.1	2.0	3.3	2.6	PD	7	14*
37	M	58	not meth	wt	GBM	B	6.0	7.0	1.9	2.0	1.9	2.0	PD	9*	12
38	F	54	not meth	wt	GBM	B	2.1	2.6	1.7	1.7	1.7	1.7	SD	9	9*
39	F	62	not meth	wt	GBM	PR	69.2	102.6	2.1	2.3	2.4	3.3	SD	7	9
40	M	42	n.a.	wt	A	B	10.8	15.4	2.1	2.1	2.3	2.2	PD	6	11*
41	F	49	not meth	wt	GBM	PR	15.6	6.9	1.9	1.8	1.9	1.8	PD	12	14

*Censored.

A = astrocytoma (WHO grade II); AA = anaplastic astrocytoma; B = biopsy; BL = baseline; CR = complete resection; EOR = extent of resection; F = female; FU = follow-up; GBM = glioblastoma; H3K27 = H3K27-mutant diffuse midline glioma; M = male; meth = MGMT promoter methylated; MGMT = O⁶-methylguanine-DNA methyltransferase; Dx = diagnosis; MTV = metabolic tumor volume; mut = mutant; n.a. = not available; NOS = not otherwise specified; PD = "progressive disease" according to RANO criteria; PFS = progression-free survival; PR = partial resection/"partial response" according to RANO criteria; res = response; SD = "stable disease" according to RANO criteria; TBR_{max}, TBR_{mean} = maximum and mean tumor-to-brain ratio; wt = wildtype.

TABLE 2
Univariate Survival Analyses Regarding General Prognostic Factors and ¹⁸F-FET PET Imaging Parameters

Parameter	Threshold	Univariate PFS analysis		Threshold	Univariate OS analysis	
		P	PFS (mo)		P	OS (mo)
MGMT promoter	Meth vs. not meth	0.010	12 vs. 8	Meth vs. not meth	0.030	21 vs. 13
EOR	CR vs. PR/B	0.458	10 vs. 8	CR vs. PR/B	0.127	22 vs. 13
Age	≤65 vs. >65 y	0.120	10 vs. 8	≤65 vs. >65 y	0.174	16 vs. 15
TBR _{mean} at baseline	1.9	0.173	11 vs. 7	1.8	0.557	22 vs. 14
TBR _{max} at baseline	2.0	0.004	11 vs. 6	1.9	0.328	17 vs. 12
MTV at baseline	28.2 mL	<0.001	11 vs. 6	13.8 mL	0.010	22 vs. 12

B = biopsy; CR = complete resection; EOR = extent of resection; meth = MGMT promoter methylated; MGMT = O⁶-methylguanine-DNA methyltransferase; MTV = metabolic tumor volume; PFS = progression-free survival; PR = partial resection; TBR_{max}, TBR_{mean} = maximum and mean tumor-to-brain ratio.

at codon 132 of IDH1 and codon 172 of IDH2 were directly sequenced as reported (41,42). The MGMT promoter methylation status was assessed by methylation-specific polymerase chain reaction, as described elsewhere (42).

Statistical Analysis

Descriptive statistics are provided as mean and SD or median and range. The Student *t* test was used to compare 2 groups. The Mann–Whitney rank-sum test was used when variables were not normally distributed. The diagnostic performance of MRI for predicting a favorable PFS and OS were calculated using 2 × 2 contingency tables; statistical significance was determined by the Pearson χ^2 test.

The prognostic value of the absolute ¹⁸F-FET PET parameters TBR_{max}, TBR_{mean}, and MTV was assessed by receiver-operating-characteristic (ROC) curve analyses using a favorable PFS and OS as reference. Favorable outcome was defined as a PFS ≥ 9 mo and an OS ≥ 15 mo. These outcome thresholds were adopted from a previous response assessment study of our group in glioblastoma patients treated with temozolomide chemoradiation (28). In that study, the median PFS was 7.2 mo and the median OS 14.1 mo, similar to the survival reported in the EORTC-NCIC 22981/26981 trial (PFS, 6.9 mo; OS, 14.6 mo) (1). Thus, slightly higher values for PFS and OS were considered as favorable outcome thresholds. Decision cutoff was considered optimal when the product of paired values for sensitivity and specificity reached

its maximum. As a measure of the test's diagnostic quality, the area under the ROC curve (AUC), its SE, and level of significance were determined. Only patients with uncensored survival data were included in ROC analyses for the evaluation of the diagnostic performance. Additionally, the value of relative changes of TBR_{max}, TBR_{mean}, and MTV to predict a significantly longer PFS and OS as an indicator for response to adjuvant TMZ was evaluated using a threshold of ≤ 0% vs. > 0%, as reported (28).

Univariate survival analyses were performed using Kaplan–Meier estimates. The log-rank test was used for comparison of the median PFS and OS between the subgroups. Patients were censored if the event (progression or death) had not occurred at the time of data evaluation (April 2020). Parameters that were significant in univariate analyses were included in multivariate models. Multivariate Cox proportional hazards models were constructed to test the relationship between relative changes of ¹⁸F-FET PET parameters and other strong prognostic factors (i.e., age, extent of resection, MGMT promoter methylation, and MTV or TBR_{max} at baseline) for a favorable survival as an indicator for response to adjuvant temozolomide chemotherapy. This analysis was done for each ¹⁸F-FET PET imaging parameter separately (i.e., for relative TBR_{max} and MTV change). Hazard ratios (HRs) and their 95% CIs were calculated.

P values of 0.05 or less were considered significant. Statistical analyses were performed using SPSS statistics (Release 25.0; SPSS Inc.).

TABLE 3
Univariate Survival Analysis Regarding Changes of Imaging Parameters During Adjuvant Temozolomide Therapy

Parameter	Threshold	Univariate PFS analysis		Univariate OS analysis	
		P	PFS (mo)	P	OS (mo)
RANO criteria	SD/PR/CR vs. PD	0.618	9 vs. 10	0.752	16 vs. 17
TBR _{mean} change	≤0% vs. >0%	0.217	10 vs. 8	0.328	17 vs. 14
TBR _{max} change	≤0% vs. >0%	0.031	11 vs. 8	0.032	24 vs. 12
MTV change	≤0% vs. >0%	0.007	11 vs. 8	0.005	29 vs. 12

CR = “complete response” according to RANO criteria; MTV = metabolic tumor volume; PD = “progressive disease” according to RANO criteria; PFS = progression-free survival; PR = “partial response” according to RANO criteria; SD = “stable disease” according to RANO criteria; TBR_{max}, TBR_{mean} = maximum and mean tumor-to-brain ratio.

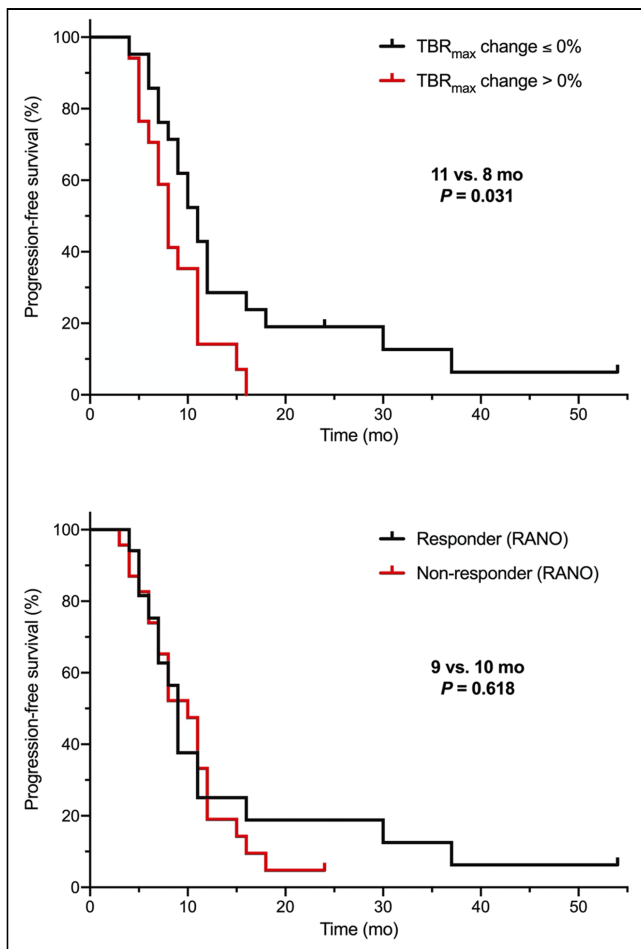


FIGURE 1. Kaplan-Meier curves for PFS separated by relative changes of TBR_{max} on ¹⁸F-FET PET (top) and RANO criteria for MRI (bottom) after 2 cycles of adjuvant temozolomide. Responders on ¹⁸F-FET PET defined by any decrease or an unchanged TBR_{max} at follow-up compared with baseline had a significantly longer PFS than nonresponders (i.e., patients with an increase of TBR_{max} at follow-up compared with baseline) (11 vs. 8 mo; *P* = 0.031). On the other hand, PFS of responders according to RANO criteria regarding MRI was not significantly longer than in nonresponders.

RESULTS

Patients

Forty-one patients (mean age, 52 ± 13 y; age range, 20–79 y; 19 women) with newly diagnosed glioma (WHO grade IV glioblastoma, IDH-wildtype, *n* = 32; WHO grade IV glioblastoma, IDH-mutant, *n* = 3; WHO grade IV glioblastoma, not otherwise specified, *n* = 2; WHO grade III anaplastic astrocytoma, IDH-wildtype, *n* = 2; WHO grade II astrocytoma, IDH-wildtype, *n* = 1; WHO grade IV H3 K27-mutant diffuse midline glioma, *n* = 1) were examined. Sixteen patients had a methylated MGMT promoter (39%), and in 11 patients a complete tumor resection (27%) could be obtained. All 41 patients completed baseline ¹⁸F-FET PET and MRI (100%). At follow-up, ¹⁸F-FET PET in combination with MRI was available in 38 patients (93%). Because of subsequent clinical deterioration, 3 of 41 (7%) patients were not able to undergo follow-up ¹⁸F-FET PET imaging. At the time of data evaluation, tumor progression, according to RANO criteria, had occurred in 37 patients (90%) and death in 33

patients (80%). In the whole cohort, the median PFS was 9 mo (range, 3–54 mo), and the median OS was 14 mo (range, 5–54 mo). Further details regarding the patient characteristics and neuroimaging findings at baseline and follow-up are shown in Table 1.

Prognostic Value of ¹⁸F-FET Imaging Parameters as Assessed by ROC Analyses

The results of ROC analyses of absolute ¹⁸F-FET PET parameters for predicting a favorable PFS of ≥ 9 mo or an OS of ≥ 15 mo are presented in Supplemental Tables 1 and 2 (supplemental materials are available at <http://jnm.snmjournals.org>). Predominantly, all ¹⁸F-FET PET parameters at baseline and follow-up significantly predicted a favorable PFS or OS (range of AUC values, 0.73–0.86). Highest accuracies (AUC ≥ 0.80) to predict a favorable PFS were observed for TBR_{max} and MTV both at baseline and at follow-up, and for MTV at follow-up to predict a favorable OS. Of these significant prognostic ¹⁸F-FET PET imaging parameters, parameters at baseline (before start of adjuvant TMZ therapy) were selected for univariate survival analyses.

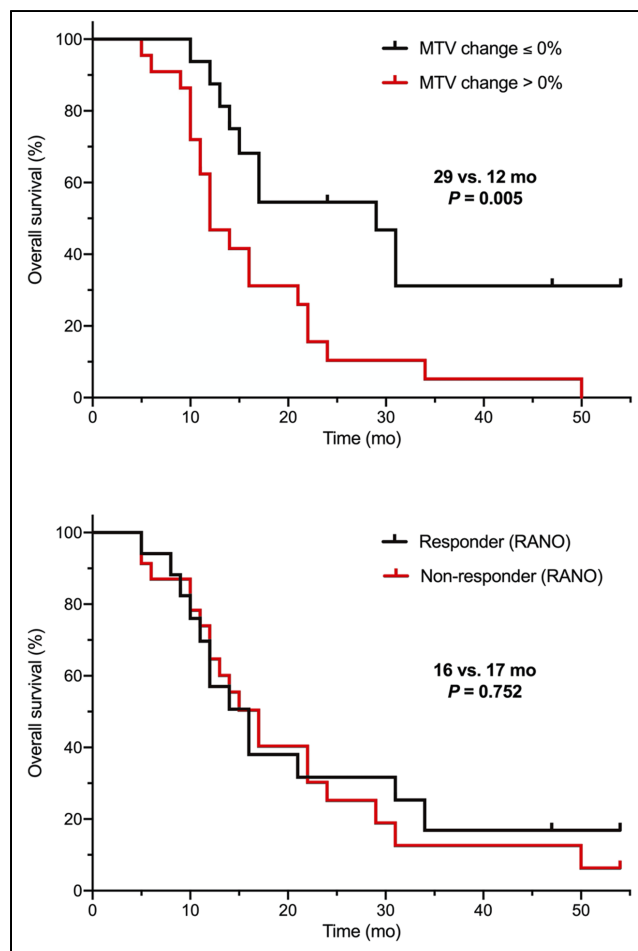


FIGURE 2. Kaplan-Meier curves for OS separated by relative MTV changes on ¹⁸F-FET PET (top) and RANO criteria for MRI (bottom) after 2 cycles of adjuvant temozolomide. Responders on ¹⁸F-FET PET defined by any decrease or an unchanged MTV at follow-up compared with baseline had a significantly 2.4-fold-longer OS than patients with an increase of MTV at follow-up compared with baseline (29 vs. 12 mo; *P* = 0.005). In contrast, OS of responders according to RANO criteria regarding MRI was not significantly longer than in nonresponders.

TABLE 4
Multivariate Survival Analysis of Changes of ¹⁸F-FET PET Imaging Parameters

Parameter	Multivariate PFS analysis			Multivariate OS analysis		
	HR	95% CI	P	HR	95% CI	P
TBR _{max} change	2.920	1.272–6.705	0.012*	2.660	1.144–6.189	0.023*
MTV change	1.925	0.842–4.404	0.121†	3.614	1.481–8.820	0.005†

*Compared with age, EOR, MGMT promoter methylation status, and TBR_{max} baseline.

†Compared with age, EOR, MGMT promoter methylation status, and MTV baseline.

MTV = metabolic tumor volume; PFS = progression-free survival; PR = partial response/partial resection; TBR_{max} = maximum tumor-to-brain ratio.

Univariate Survival Analyses Regarding Baseline Prognostic Factors and ¹⁸F-FET PET Imaging Parameters

Patients with completely resected tumors or an age ≤ 65 y had no significantly longer PFS or OS (Table 2). In contrast, patients with MGMT promoter–methylated tumors had a significantly longer PFS (12 vs. 8 mo; *P* = 0.010) and OS (21 vs. 13 mo; *P* = 0.030) (Table 2). Regarding ¹⁸F-FET PET parameters, patients with an absolute MTV of ≤ 28.2 mL or a TBR_{max} ≤ 2.0 at baseline had an almost doubled PFS (both 11 vs. 6 mo; *P* < 0.001 and *P* = 0.004, respectively). Additionally, an absolute MTV of ≤ 13.8 mL at baseline predicted a significantly longer OS (22 vs. 12 mo; *P* = 0.010) (Table 2).

Univariate Survival Analysis Regarding Changes of Imaging Parameters During Adjuvant TMZ Therapy

After application of 2 cycles of adjuvant TMZ, relative changes of TBR_{max} and MTV predicted a significantly (*P* = 0.031 and 0.007, respectively) longer PFS (both 11 vs. 8 mo) (Table 3). Relative changes of TBR_{max} and MTV after 2 cycles of adjuvant TMZ predicted also a significantly longer OS (24 vs. 12 mo; *P* = 0.032, and 29 vs. 12 mo; *P* = 0.005) (Table 3). Conversely, both the PFS and OS in responding patients on MRI (i.e., MRI findings consistent with *Stable Disease* or *Partial Response* according to RANO) was not significantly prolonged (9 vs. 10 mo; *P* = 0.618, and 16 vs. 17 mo; *P* = 0.752) (Figs. 1 and 2).

Multivariate Survival Analysis Regarding Changes of Imaging Parameters During Adjuvant TMZ Therapy

A TBR_{max} reduction was a significant parameter in the multivariate survival analysis (*P* = 0.012; HR, 2.920; 95% CI, 1.272–6.705), which predicts a significantly longer PFS (Table 2) independent of age, extent of resection, MGMT promoter methylation, and TBR_{max} at baseline. Furthermore, relative reductions of both TBR_{max} and MTV after 2 cycles of adjuvant TMZ predicted significantly longer OS (Table 4). A change of MTV after 2 cycles of adjuvant TMZ was the most significant parameter independent of age, extent of resection, MGMT promoter methylation, and MTV at baseline (*P* = 0.005; HR, 3.614; 95% CI, 1.481–8.820). Thus, a decrease of these ¹⁸F-FET PET parameters appears to be associated with response to adjuvant temozolomide chemotherapy.

DISCUSSION

The main finding of the present study is that relative changes of MTV and TBR_{max} obtained from ¹⁸F-FET PET provide valuable clinical information on tumor response to adjuvant TMZ after

completion of radiotherapy with concurrent TMZ in patients with newly diagnosed glioma. Importantly, this information cannot be derived from an MRI response assessment based on RANO criteria. In contrast to MRI, relative MTV and TBR_{max} changes predicted both a significantly longer PFS (≥9 mo) and a significantly longer OS (≥15 mo), indicating that ¹⁸F-FET PET is a powerful tool for the evaluation of treatment effects. Moreover, prediction of response to adjuvant TMZ using these ¹⁸F-FET PET parameters was possible irrespective of MGMT promoter methylation and other strong prognostic factors. Thus, our data suggest that ¹⁸F-FET PET is highly sensitive in the early response assessment of adjuvant TMZ, which could be useful for patient management, for example, the diagnosis of pseudoprogression or reevaluation of other treatment options in the case of early tumor progression (Fig. 3). Furthermore, for the patient, the patient's relatives, and the treating physician it is of great importance whether a favorable or unfavorable clinical course can be expected. Moreover, on the basis of the response assessment, treatment decisions may be facilitated, for example, an earlier change to a second-line therapy.

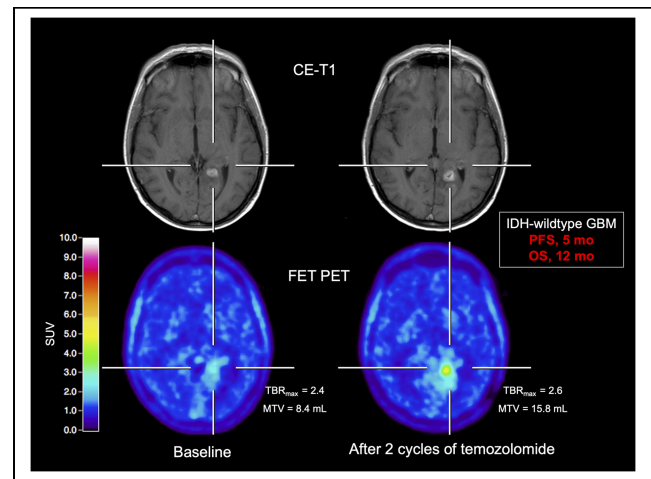


FIGURE 3. Patient with an IDH-wildtype glioblastoma (GBM) with unfavorable survival (patient 8). After 2 cycles of adjuvant temozolomide chemotherapy, the contrast-enhancing lesion on MRI is slightly enlarged (criterion *progressive disease* according to RANO criteria not fulfilled) compared with baseline MRI (upper row). In contrast, corresponding ¹⁸F-FET PET at follow-up shows relative to baseline scan (bottom row) an increase of metabolic activity as assessed by TBR_{max} and MTV (relative increase, 8% and 88%, respectively). Patient had unfavorable outcome with a PFS of 5 mo and an OS of 12 mo.

Our findings are in line with a previous study assessing the evaluation of response to radiotherapy in glioblastoma patients. That prospective study evaluated the predictive value of early TBR changes of ^{18}F -FET uptake after postoperative radiotherapy with concurrent TMZ in patients with newly diagnosed glioblastoma (28,30). ^{18}F -FET PET was performed at baseline (before chemoradiation) and early after chemoradiation completion (i.e., after 7–10 d and 6–8 wk later). One main finding of that study was that a relative decrease of TBRs related to radiotherapy with concurrent TMZ was associated with a significantly longer survival (i.e., PFS and OS). Furthermore, and consistent with our findings, the authors observed that ^{18}F -FET PET tumor volume changes (MTV) relative to baseline were also associated with a significantly longer OS. However, in that study, the value of ^{18}F -FET PET for the evaluation of effects to adjuvant TMZ after chemoradiation completion was not assessed. In addition to the latter study evaluating the effects of radiotherapy with concurrent TMZ on ^{18}F -FET PET parameters and survival (28,30), we here observed the additional value of relative MTV change for the prediction of response to adjuvant TMZ chemotherapy.

The value of the relative MTV change has also been reported for the evaluation of the effects of other neurooncologic treatment options such as antiangiogenic therapy. In a prospective study by Schwarzenberg et al., predominantly heavily pretreated progressive glioma patients underwent bevacizumab and irinotecan therapy. They were examined using standard MRI and 3,4-dihydroxy-6- ^{18}F fluoro-L-phenylalanine (^{18}F -FDOPA) amino acid PET at baseline and early after starting the therapy (i.e., after 2 wk and after 6 wk) (43). Consistent with our study, the relative ^{18}F -FDOPA MTV change relative to baseline after bevacizumab and irinotecan predicted a significantly prolonged OS. Additionally, a prospective study by our group has also highlighted the value of MTV for the evaluation of response to bevacizumab plus lomustine (44). In that study, IDH-wildtype glioblastoma patients at first progression were treated with bevacizumab plus lomustine. Contrast-enhanced MRI and ^{18}F -FET PET were performed at baseline and follow-up after 8–10 wk. Again, relative MTV changes enabled an OS prediction early after treatment initiation.

Furthermore, the predictive value of relative MTV changes has also been reported in patients with nonenhancing WHO grade II or III glioma treated with alkylating chemotherapy (TMZ or lomustine plus procarbazine) (26).

CONCLUSION

^{18}F -FET PET-derived imaging parameters can be used to predict response to adjuvant TMZ chemotherapy and may thus provide important information concerning the patient's PFS and OS. In particular, parameters derived from ^{18}F -FET PET, such as relative MTV changes, appear to be a powerful tool for identifying responders to adjuvant TMZ early after treatment initiation irrespective of MGMT promoter methylation. Our results suggest that ^{18}F -FET PET is a valuable diagnostic tool for treatment monitoring including response assessment and justifies its use in clinical routine. An important next step to evaluate the additional clinical value of ^{18}F -FET PET is the monitoring of newer treatment options such as targeted therapy or immunotherapy, ideally in a prospective setting.

DISCLOSURE

The Wilhelm-Sander Stiftung, Germany, supported this work. No other potential conflict of interest relevant to this article was reported.

ACKNOWLEDGMENTS

All subjects gave prior written informed consent for their participation in the ^{18}F -FET PET study and evaluation of their data for scientific purposes. The local ethics committee approved the evaluation of retrospectively collected neuroimaging data. All procedures performed in studies involving human participants followed the national ethical standards and the Declaration of Helsinki.

KEY POINTS

QUESTION: Is ^{18}F -FET PET superior to conventional MRI for predicting a significantly longer survival early after adjuvant temozolomide chemotherapy initiation?

PERTINENT FINDINGS: The response to adjuvant temozolomide chemotherapy was evaluated in 41 newly diagnosed and histomolecularly defined glioma patients using ^{18}F -FET PET and contrast-enhanced MRI. Already after 2 cycles, uni- and multivariate survival analyses revealed that a reduction of ^{18}F -FET PET parameters compared with the baseline scan predicted a significantly longer PFS and OS whereas standard MRI response criteria were not significant.

IMPLICATIONS FOR PATIENT CARE: In contrast to conventional MRT, changes of ^{18}F -FET PET parameters appear to be helpful for identifying responders after 2 cycles of temozolomide chemotherapy, which could be useful for patient management such as the diagnosis of pseudoprogression or reevaluation of other treatment options.

REFERENCES

1. Stupp R, Mason WP, van den Bent MJ, et al. Radiotherapy plus concomitant and adjuvant temozolomide for glioblastoma. *N Engl J Med*. 2005;352:987–996.
2. Weller M, Butowski N, Tran DD, et al. Rindopepimut with temozolomide for patients with newly diagnosed, EGFRvIII-expressing glioblastoma (ACTIV): a randomised, double-blind, international phase 3 trial. *Lancet Oncol*. 2017;18:1373–1385.
3. Chinot OL, Wick W, Mason W, et al. Bevacizumab plus radiotherapy-temozolomide for newly diagnosed glioblastoma. *N Engl J Med*. 2014;370:709–722.
4. Stupp R, Taillibert S, Kanner AA, et al. Maintenance therapy with tumor-treating fields plus temozolomide vs temozolomide alone for glioblastoma: a randomized clinical trial. *JAMA*. 2015;314:2535–2543.
5. Stupp R, Taillibert S, Kanner A, et al. Effect of tumor-treating fields plus maintenance temozolomide vs maintenance temozolomide alone on survival in patients with glioblastoma: a randomized clinical trial. *JAMA*. 2017;318:2306–2316.
6. Herrlinger U, Tzaridis T, Mack F, et al. Lomustine-temozolomide combination therapy versus standard temozolomide therapy in patients with newly diagnosed glioblastoma with methylated MGMT promoter (CeTeG/NOA-09): a randomised, open-label, phase 3 trial. *Lancet*. 2019;393:678–688.
7. Wen PY, Macdonald DR, Reardon DA, et al. Updated response assessment criteria for high-grade gliomas: response assessment in neuro-oncology working group. *J Clin Oncol*. 2010;28:1963–1972.
8. Macdonald DR, Cascino TL, Schold SC Jr, Cairncross JG. Response criteria for phase II studies of supratentorial malignant glioma. *J Clin Oncol*. 1990;8:1277–1280.
9. Dhermain FG, Hau P, Lanfermann H, Jacobs AH, van den Bent MJ. Advanced MRI and PET imaging for assessment of treatment response in patients with gliomas. *Lancet Neurol*. 2010;9:906–920.
10. Ahluwalia MS, Wen PY. Antiangiogenic therapy for patients with glioblastoma: current challenges in imaging and future directions. *Expert Rev Anticancer Ther*. 2011;11:653–656.
11. Kumar AJ, Leeds NE, Fuller GN, et al. Malignant gliomas: MR imaging spectrum of radiation therapy- and chemotherapy-induced necrosis of the brain after treatment. *Radiology*. 2000;217:377–384.
12. Taal W, Brandsma D, de Bruin HG, et al. Incidence of early pseudo-progression in a cohort of malignant glioma patients treated with chemoradiation with temozolomide. *Cancer*. 2008;113:405–410.

13. Brandsma D, Stalpers L, Taal W, Sminia P, van den Bent MJ. Clinical features, mechanisms, and management of pseudoprogression in malignant gliomas. *Lancet Oncol*. 2008;9:453–461.
14. Galldiks N, Kocher M, Langen KJ. Pseudoprogression after glioma therapy: an update. *Expert Rev Neurother*. 2017;17:1109–1115.
15. Stuplich M, Hadizadeh DR, Kuchelmeister K, et al.. Late and prolonged pseudoprogression in glioblastoma after treatment with lomustine and temozolomide. *J Clin Oncol*. 2012;30:e180–e183.
16. Kebir S, Fimmers R, Galldiks N, et al.. Late pseudoprogression in glioblastoma: diagnostic value of dynamic O-(2-[¹⁸F]fluoroethyl)-L-tyrosine PET. *Clin Cancer Res*. 2016;22:2190–2196.
17. Shah AH, Snelling B, Bregy A, et al.. Discriminating radiation necrosis from tumor progression in gliomas: a systematic review what is the best imaging modality? *J Neurooncol*. 2013;112:141–152.
18. Hutterer M, Ebner Y, Riemenschneider MJ, et al.. Epileptic activity increases cerebral amino acid transport assessed by ¹⁸F-Fluoroethyl-L-Tyrosine amino acid PET: a potential brain tumor mimic. *J Nucl Med*. 2017;58:129–137.
19. Lescher S, Schniewindt S, Jurcoane A, Senft C, Hattingen E. Time window for post-operative reactive enhancement after resection of brain tumors: less than 72 hours. *Neurosurg Focus*. 2014;37:E3.
20. Langen KJ, Galldiks N, Hattingen E, Shah NJ. Advances in neuro-oncology imaging. *Nat Rev Neurol*. 2017;13:279–289.
21. Galldiks N, Law I, Pope WB, Arbizu J, Langen KJ. The use of amino acid PET and conventional MRI for monitoring of brain tumor therapy. *Neuroimage Clin*. 2016;13:386–394.
22. Albert NL, Weller M, Suchorska B, et al.. Response Assessment in Neuro-Oncology working group and European Association for Neuro-Oncology recommendations for the clinical use of PET imaging in gliomas. *Neuro-oncol*. 2016;18:1199–1208.
23. Galldiks N, Langen KJ, Albert NL, et al.. PET imaging in patients with brain metastasis-report of the RANO/PET group. *Neuro-oncol*. 2019;21:585–595.
24. Roelcke U, Wyss MT, Nowosielski M, et al.. Amino acid positron emission tomography to monitor chemotherapy response and predict seizure control and progression-free survival in WHO grade II gliomas. *Neuro-oncol*. 2016;18:744–751.
25. Wyss M, Hofer S, Bruhlmeier M, et al.. Early metabolic responses in temozolomide treated low-grade glioma patients. *J Neurooncol*. 2009;95:87–93.
26. Suchorska B, Unterrainer M, Biczok A, et al.. ¹⁸F-FET-PET as a biomarker for therapy response in non-contrast enhancing glioma following chemotherapy. *J Neurooncol*. 2018;139:721–730.
27. Galldiks N, Rapp M, Stoffels G, et al.. Response assessment of bevacizumab in patients with recurrent malignant glioma using [¹⁸F]fluoroethyl-L-tyrosine PET in comparison to MRI. *Eur J Nucl Med Mol Imaging*. 2013;40:22–33.
28. Galldiks N, Langen K, Holy R, et al.. Assessment of treatment response in patients with glioblastoma using [¹⁸F]Fluoroethyl-L-tyrosine PET in comparison to MRI. *J Nucl Med*. 2012;53:1048–1057.
29. Suchorska B, Jansen NL, Linn J, et al.. Biological tumor volume in 18FET-PET before radiochemotherapy correlates with survival in GBM. *Neurology*. 2015;84:710–719.
30. Piroth MD, Pinkawa M, Holy R, et al.. Prognostic value of early [¹⁸F]fluoroethyltyrosine positron emission tomography after radiochemotherapy in glioblastoma multiforme. *Int J Radiat Oncol Biol Phys*. 2011;80:176–184.
31. Ellingson BM, Bendszus M, Boxerman J, et al.. Consensus recommendations for a standardized brain tumor imaging protocol in clinical trials. *Neuro-oncol*. 2015;17:1188–1198.
32. Hamacher K, Coenen HH. Efficient routine production of the ¹⁸F-labelled amino acid O-2-¹⁸F fluoroethyl-L-tyrosine. *Appl Radiat Isot*. 2002;57:853–856.
33. Law I, Albert NL, Arbizu J, et al.. Joint EANM/EANO/RANO practice guidelines/SNMMI procedure standards for imaging of gliomas using PET with radiolabelled amino acids and [¹⁸F]FDG: version 1.0. *Eur J Nucl Med Mol Imaging*. 2019;46:540–557.
34. Herzog H, Langen KJ, Weirich C, et al.. High resolution BrainPET combined with simultaneous MRI. *Nuklearmedizin*. 2011;50:74–82.
35. Lohmann P, Herzog H, Rota Kops E, et al.. Dual-time-point O-(2-[(¹⁸F]fluoroethyl)-L-tyrosine PET for grading of cerebral gliomas. *Eur Radiol*. 2015;25:3017–3024.
36. Pauleit D, Floeth F, Hamacher K, et al.. O-(2-[¹⁸F]fluoroethyl)-L-tyrosine PET combined with MRI improves the diagnostic assessment of cerebral gliomas. *Brain*. 2005;128:678–687.
37. Galldiks N, Stoffels G, Filss C, et al.. The use of dynamic O-(2-¹⁸F-fluoroethyl)-L-tyrosine PET in the diagnosis of patients with progressive and recurrent glioma. *Neuro-oncol*. 2015;17:1293–1300.
38. Louis DN, Perry A, Reifenberger G, et al.. The 2016 World Health Organization classification of tumors of the central nervous system: a summary. *Acta Neuropathol (Berl)*. 2016;131:803–820.
39. Capper D, Zentgraf H, Balss J, Hartmann C, von Deimling A. Monoclonal antibody specific for IDH1 R132H mutation. *Acta Neuropathol (Berl)*. 2009;118:599–601.
40. Capper D, Weissert S, Balss J, et al.. Characterization of R132H mutation-specific IDH1 antibody binding in brain tumors. *Brain Pathol*. 2010;20:245–254.
41. Hartmann C, Hentschel B, Wick W, et al.. Patients with IDH1 wild type anaplastic astrocytomas exhibit worse prognosis than IDH1-mutated glioblastomas, and IDH1 mutation status accounts for the unfavorable prognostic effect of higher age: implications for classification of gliomas. *Acta Neuropathol (Berl)*. 2010;120:707–718.
42. Felsberg J, Rapp M, Loeser S, et al.. Prognostic significance of molecular markers and extent of resection in primary glioblastoma patients. *Clin Cancer Res*. 2009;15:6683–6693.
43. Schwarzenberg J, Czernin J, Cloughesy TF, et al.. Treatment response evaluation using ¹⁸F-FDOPA PET in patients with recurrent malignant glioma on bevacizumab therapy. *Clin Cancer Res*. 2014;20:3550–3559.
44. Galldiks N, Dunkl V, Ceccon G, et al.. Early treatment response evaluation using FET PET compared to MRI in glioblastoma patients at first progression treated with bevacizumab plus lomustine. *Eur J Nucl Med Mol Imaging*. 2018;45:2377–2386.